THE JOURNAL OF PHYSICAL CHEMISTRY C

Article

pubs.acs.org/JPCC

Polymer-Capped Sulfur Copolymers as Lithium–Sulfur Battery Cathode: Enhanced Performance by Combined Contributions of Physical and Chemical Confinements

Shuaibo Zeng,[†] Ligui Li,*[,†,‡] Dengke Zhao,[†] Ji Liu,[†] Wenhan Niu,[†] Nan Wang,[†] and Shaowei Chen*[,†,§]

[†]New Energy Research Institute, College of Environment and Energy, South China University of Technology, Guangzhou Higher Education Mega Center, Guangzhou 510006, China

[‡]Guangdong Provincial Key Laboratory of Atmospheric Environment and Pollution Control, College of Environment and Energy, South China University of Technology, Guangzhou 510006, China

[§]Department of Chemistry and Biochemistry, University of California, 1156 High Street, Santa Cruz, California 95064, United States

Supporting Information

ABSTRACT: Flexible polymers show high potential applications in rechargeable lithium–sulfur (Li–S) batteries for their capability of confining sulfur diffusion and tolerance to large volume expansion during lithiation. Herein, sulfur is copolymerized with 3-butylthiophene via radical polymerization by heating the mixture of both components at controlled temperatures. Further capping of the thus-synthesized copolymer CP(S3BT) with highly conductive PEDOT:PSS thin film substantially enhances the electrical conductivity. With the resulting polymer hybrids as the cathode material, a Li–S battery is constructed which shows an initial discharge capacity of 1362 mA h g^{-1} at 0.1 C and a reversible capacity of 631 mA h g^{-1} even at 5 C. Moreover, the polymer cathode exhibits a high capacity of 682 mA h g^{-1} after 500 charge–discharge cycles at 1 C with 99.947% retention per cycle. The remarkable performance is attributed to the synergetic effects of (i) high conductivity resulting from both the conducting blocks of poly(3-butylthiophene) (P3BT) and PEDOT:PSS capping layer, (ii) physical confinement of polysulfides by P3BT segments and PEDOT:PSS capping layers, and (iii) chemical confinement resulting from the high density of chemical bonds between sulfur and 3-butylthiophene. The results may offer a new paradigm in the development of efficient and stable polymer cathodes for high performance Li–S batteries.

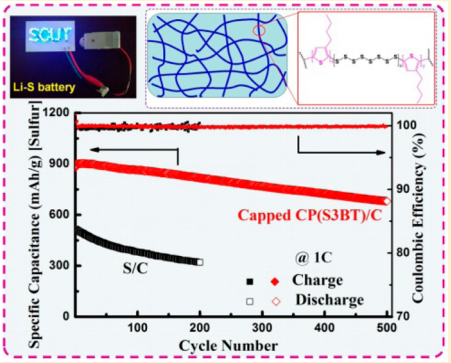

1. INTRODUCTION

The rechargeable lithium–sulfur (Li–S) battery has been attracting great attention due to its high theoretical specific capacity of 1672 mA h g^{-1} and energy density of 2600 kW kg^{-1}, which can meet the requirements of advanced energy storage systems.[1,2] Sulfur is an earth-abundant element. Desulfuration of fossil fuels in petroleum refining and pretreatment of fire coal also provide a massive amount of sulfur every year.[3] Moreover, sulfur is inexpensive and environmentally friendly. These unique characteristics render Li–S batteries one of the most promising candidates for next-generation high performance energy storage systems.[4,5]Yet the practical applications of Li–S batteries are impeded by several serious problems such as poor cycling performance, low Coulombic efficiency and limited *C*-rate capacity,[1,6] which are primarily ascribed to poor electric conductivity of sulfur and polysulfides (~5×10^{-30} S/cm at 25 °C),[7,8] large volume expansion (up to 80%) of sulfur after lithiation,[9,10] dissolution, and the so-called "shuttle" effect of lithium polysulfides (Li_2S_8, Li_2S_6, Li_2S_4, and Li_2S_2) in organic electrolytes.[11−15]

Thus, substantial efforts have been devoted to mitigating these issues. For example, to impede the dissolution of lithium polysulfides, encapsulation of sulfur/polysulfides has been extensively studied, for instance, by using porous carbon nanofibers,[16−18] TiO_2 yolk–shell nanoarchitectures,[10,19] sandwich-type architecture,[20,21] layered porous carbon,[22,23] carbon nanotubes,[15,24,25] graphene,[26−29] polymers,[30−34] and metal oxides,[35,36] leading to improved cycling stability of Li–S batteries.[34] However, these methods mostly resort to physical confinement where the interactions between sulfur and the encapsulating materials do not involve covalent bonding but only weak physical adsorption.[37] To further advance the performance of the Li–S battery, effective encapsulation of sulfur and polysulfides with both physical confinement and chemical cross-linking are highly desired.

Due to the high flexibility and easy functionalization, conducting polymers have been used extensively in Li–S

Received: September 21, 2016
Revised: November 25, 2016
Published: January 13, 2017

DOI: 10.1021/acs.jpcc.6b09543
J. Phys. Chem. C 2017, 121, 2495−2503

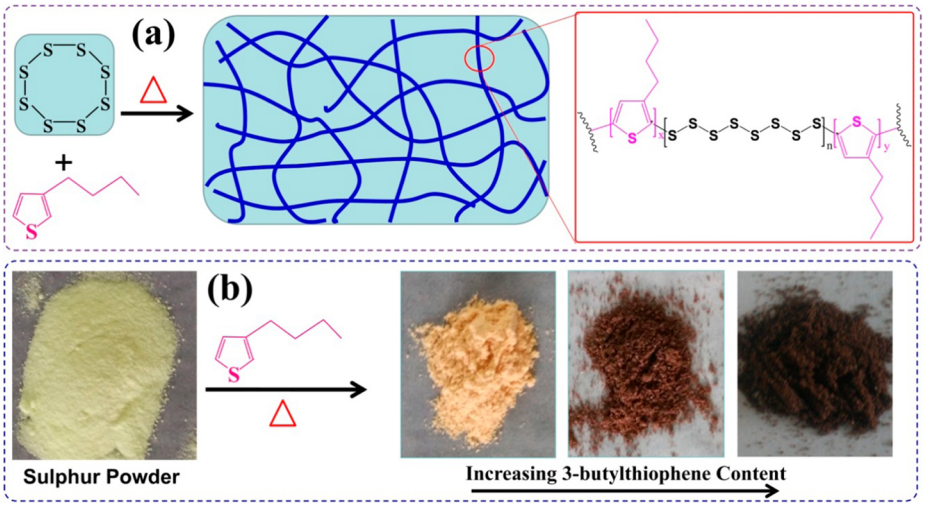

Figure 1. (a) Reaction scheme of the synthesis of CP(S3BT) and (b) images showing the color evolution during sample preparation.

battery to confine sulfur. For instance, Oschmann et al. reported covalent bonding of sulfur to preformed poly(3-hexylthiophene-2,5-diyl) (P3HT) by radical reaction of sulfur and the allyl end groups on P3HT. Utilizing the obtained product as an additive to sulfur cathode in an Li−S battery, the phase separation between P3HT and sulfur was substantially reduced, leading to enhanced cycling stability and *C*-rate performance, as compared to that of simple mixtures of sulfur and P3HT.[38] However, several drawbacks remained. For example, as the number of allyl terminal groups on P3HT was very limited, only a small quantity of sulfur was covalently bonded to the P3HT main chains and effectively constrained, while most of the loaded sulfur in electrode was noncovalently bonded, which might be easily dissolved into electrolyte during cycling and cause an irreversible loss of active sulfur and hence capacity decay. In view of these shortcomings, one immediate question arises. Is it possible to homogeneously/randomly copolymerize 3-alkyl thiophene directly with sulfur so that interconnecting and homogeneous polythiophene conducting networks can be *in situ* formed for charge transfer, and concurrently, sulfur is effectively confined by polymer networks? This is the primary motivation of the present work.

Herein, random copolymerization of sulfur and 3-butylthiophene was realized by simple heating of their mixtures. The thus-prepared bulk copolymer was further capped with a PEDOT:PSS layer and used as the active material for the cathode of Li−S battery. Such polymer cathode exhibited a remarkable electrochemical performance, with an initial discharge capacity of 1362 mA h g^{-1} at 0.1 C, a reversible capacity of 631 mA h g^{-1} at a large current density of 5 C, and a specific capacity of 682 mA h g^{-1} even after 500 cycles at 1 C with a decay rate of only 0.053% per cycle. To the best of our knowledge, these capacity values are the highest that have been ever reported for polymer cathodes in Li−S battery. This was attributed to the formation of cross-linking networks with numerous covalent bonds between sulfur and 3-butylthiophene in the P3BT backbone, which together with the PEDOT:PSS capping layer effectively impeded the dissolution and diffusion of polysulfides. Furthermore, the PEDOT:PSS coating enhanced the electrical conductivity, leading to a dramatic improvement of the capacitance of the Li−S battery.

2. EXPERIMENTAL SECTION

2.1. Preparation of CP(S3BT). CP(S3BT) was prepared by bulk copolymerization of 3-butylthiophene with sulfur. Typically, 4 g of sulfur powders in a glass beaker was gradually heated up to 170 °C to form a clear yellow liquid, into which was then added 1.7 g of 3-butylthiophene in a dropwise fashion under magnetic stirring. The polymerization was allow to proceed at 170 °C for 5 h before the mixture was cooled down to room temperature, which resulted in the formation of a glass-like brown solid, the CP(S3BT) copolymer with 70 wt % of elemental S at the starting mixture. For comparison, a control sample CP(S3BT)-80 copolymer containing 80 wt % of elemental S in the starting mixtures was also prepared in a similar fashion and referred to as CP(S3BT)-80. For clarity, the CP(S3BT) sample throughout the present work contains 70 wt % sulfur unless otherwise indicated.

2.2. Characterization. The phase separation of the materials was characterized by an Olympus optical microscope (OM). Scanning electron microscopy (SEM) and transmission electron microscopy (TEM) measurements were conducted on a Hitachi S-4800 field emission scanning electron microscopy (FESEM) and a JEOL JEM-2100 transmission electron microscopy (TEM) at an acceleration voltage of 200 kV, respectively. XRD measurements were performed on Bruker D8 using Cu Kα radiation. FTIR spectra were acquired with a Nicolet 6700 infrared spectrometer using KBr pellets in the transmission mode. X-ray photoelectron spectroscopy (XPS) measurements were carried out on a Phi X-tool XPS instrument. The glass transition temperature was determined with a TAQ20 differential scanning calorimeter (DSC) at a heating rate of 3 °C min^{-1}. Thermogravimetric analysis (TGA) was conducted on a METTLER instrument under N_2 atm at a heating rate of 10 °C min^{-1}. For electric conductivity measurements, the powder materials were compressed at 40 MPa to form circular sheets with the same diameter using a tablet compression machine. The electric conductivity was measured on a KEITHLEY 2636B source-meter using the two-probe method.

2.3. Coin−Cell Fabrication and Battery Tests. In brief, the polyvinylidene fluoride (PVDF) binder was completely dissolved in *N*-methyl-2-pyrrolidene (NMP) under magnetic stirring, The CP(S3BT) prepared above and conductive carbon black were added into the solution to form a homogeneous

DOI: 10.1021/acs.jpcc.6b09543
J. Phys. Chem. C 2017, 121, 2495−2503

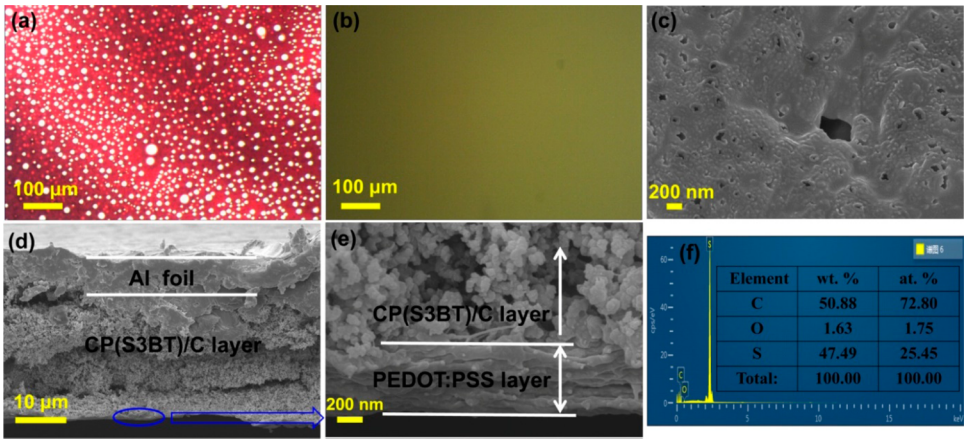

Figure 2. (a, b) Optical microscopy images of (a) a simple mixture of elemental sulfur and P3BT and (b) CP(S3BT). (c) SEM image of CP(S3BT). (d) Cross section SEM image of the cathode. (e) High-magnification SEM image of the blue oval area in part d. (f) EDS spectrum and elemental contents of the CP(S3BT)/C layer in part d.

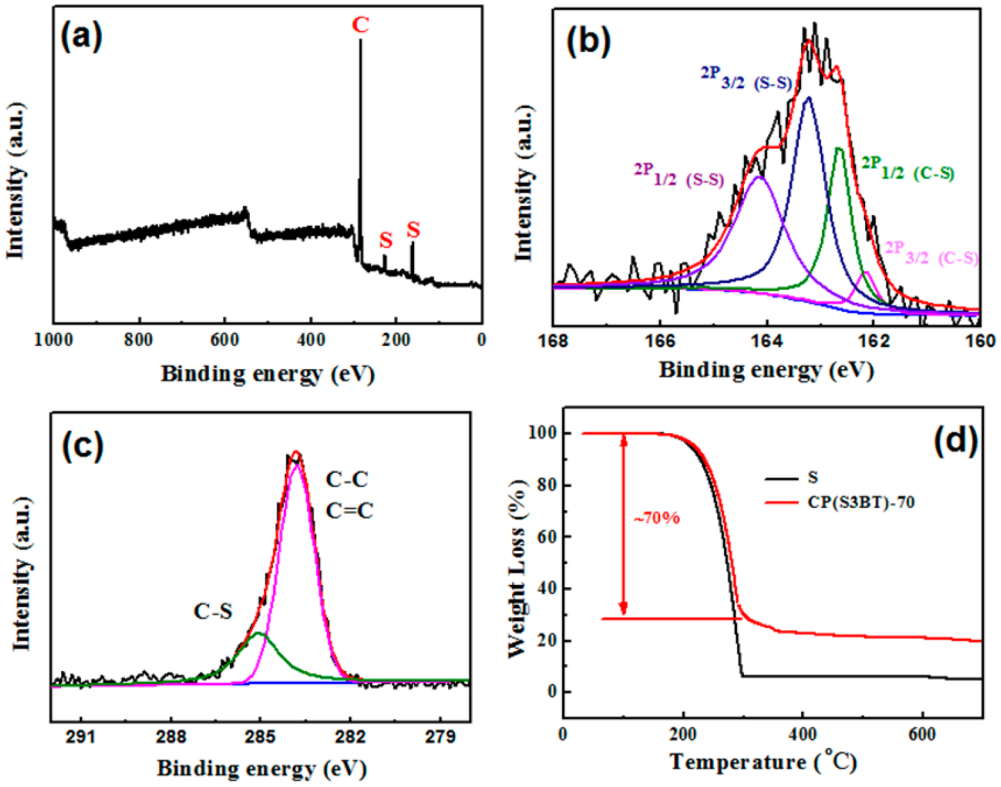

Figure 3. (a) XPS survey spectrum of CP(S3BT),and the corresponding high-resolution scans of (b) S 2p and (c) C 1s electrons, where black curves are experimental data and colored curves are the deconvolution fits. (d) TGA curves of pure sulfur and CP(S3BT) measured under a N_2 flow at a heating rate of 10 °C min^{-1} from 30 to 900 °C.

slurry at a mass ratio of CP(S3BT):conductive carbon black:PVDF = 65:25:10. Subsequently, the slurry was capped on an aluminum current collector using the doctor blade method and then dried at 60 °C for 18 h in a vacuum oven. The obtained cathode foil was pressed and cut into circular sheets at a diameter of 12 mm, and further capped with a thin layer of PEDOT:PSS by drop casting. The typical mass loading of active sulfur was calculated to be 1.0 mg cm^{-2}. The CR2032-type experiment cells were assembled in an argon-filled glovebox. The cell comprised of a positive electrode, a diaphragm Celgard 2400 as the separator, a lithium foil as the reference/counter electrode, and the mixed solution of 1,3-dioxolane and 1,2-dimethoxyethane (v:v 1:1) containing 1 M lithium bis(trifluoromethanesulfonyl) imide (LiTFSI), and 0.1 M $LiNO_3$ as the electrolyte. Conventional sulfur cathodes were also prepared according to the same procedure at a mass ratio of 40:50:10. Galvanostatic discharge−charge tests on the as-fabricated cells were performed by potential cycling between 1.5 and 3.0 V (vs Li/Li^+) at different current rates using a button cell test system (LANHE CT2001A 5 V 50 mA). Cyclic voltammetry (CV) studies were performed in the potential range of 1.5 to 3.0 V at varied scan rates. Electrochemical impedance spectroscopy (EIS) studies were performed at the

DOI: 10.1021/acs.jpcc.6b09543
J. Phys. Chem. C 2017, 121, 2495−2503

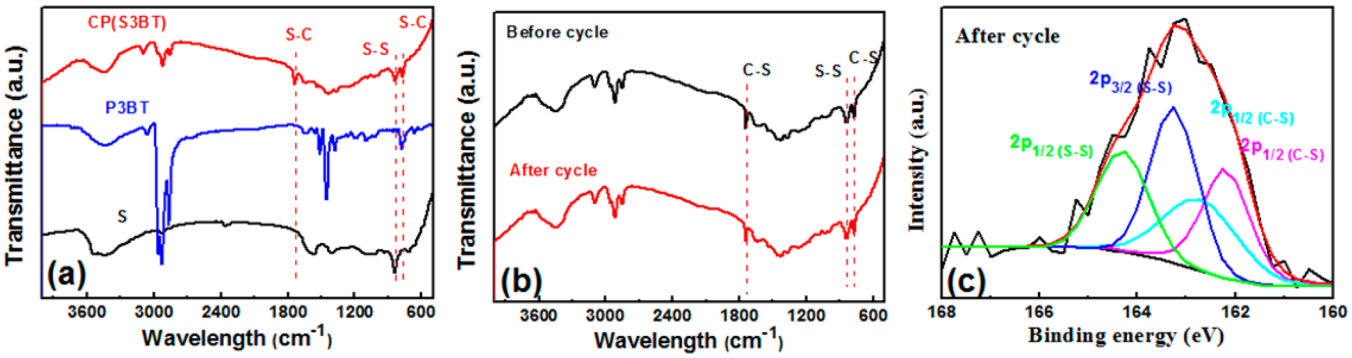

Figure 4. (a) FTIR spectra of CP(S3BT), P3BT and S before discharge−charge cycling. (b) FTIR spectra of CP(S3BT) before and after 500 discharge−charge cycles at 1 C. (c) High-resolution XPS spectrum of the S 2p electrons in CP(S3BT) after 500 discharge−charge cycles at 1 C.

charged state within the frequency range of 100 kHz to 10 mHz at an ac amplitude of 5 mV.

3. RESULTS AND DISCUSSION

During copolymerization, molten elemental sulfur (S_8) was mixed with 3-butylthiophene that had a relatively high boiling point of 182 °C. To efficiently open the ring in S_8 and form a high concentration of diradicals, bulk copolymerization was conducted at 170 °C.[3,39] The preparation process of CP(S3BT) was illustrated in Figure 1a, which involved the following two steps: (i) ring opening of S_8 to produce sulfur diradicals at 170 °C; and (ii) 3-butylthiophene was injected into the clear orange liquid sulfur to initiate copolymerization of 3-butylthiophene and S_8 diradicals at 170 °C. The formation of regioregular random P3BT in this process was supported by the appearance of a glass transition (T_g) of −12 °C as determined by DSC measurements (Figure S1). In addition, the color of finally obtained solid changed from yellow to dark brown with an increasing content of 3-butylthiophene in the starting mixture (Figure 1b), again indicative of the formation of copolymers of sulfur and 3-butylthiophene.

Figure 2 depicted the morphology of the cathode active materials. For the conventional cathode based on a simple mixture of elemental sulfur and P3BT, sulfur particles of tens of microns in diameter were observed (Figure 2a), because of large-scale phase separation between sulfur and P3BT. In sharp contrast, no distinct particles but a homogeneous and featureless film were observed in the CP(S3BT) sample (Figure 2b). SEM images in Figure 2c showed that the CP(S3BT) film was composed of nanoscale granular domains seemingly covered by a thin polymer layer. Further increasing the sulfur content to 80% led to phase separation (Figure S2), which is not beneficial to the enhancement of device performance as shown below. Figure 2d depicts the SEM image of the cross-section of the CP(S3BT)-based cathode, where the thickness of the CP(S3BT)/C layer was estimated to be about 15 μm. In the higher-magnification SEM image of the area indicated by a blue ellipse in Figure 2d, a PEDOT:PSS coating layer of ca. 500 nm in thickness was observed (Figure 2e). In addition, the domains with granular shapes of ca. 100 nm in diameter were found to be homogeneously distributed in the CP(S3BT)/C layer. In the corresponding high-resolution TEM images shown in Figure S3, it can be seen that such domains were comprised of many small particles of tens of nanometers in diameter. Moreover, well-defined lattice fringes with *d*-spacings of 0.26, 0.24, and 0.196 nm can be seen in these nanoparticles, which are consistent with the (333), (244), and (515) planes of crystalline sulfur (PDF#08−0247), respectively.[40] These observations again signified the successful suppression of phase separation between sulfur and P3BT via forming radical copolymers of sulfur and 3-butylthiophene. In the corresponding EDS analysis of the CP(S3BT)/C layer (Figure 2f), the S element content was found to be 47.49 wt %, which is close to the theoretical value (45.5 wt %). Taken together, the above observations indicate the successful preparation of a bulk copolymer film consisting of sulfur nanoparticles and 3-butylthiophene through radical polymerization.

The elemental compositions and valence states in CP(S3BT) were then investigated by XPS studies. In the survey spectrum depicted in Figure 3a, the C 1s, S 2s, and S 2p electrons can be clearly identified. In the high resolution scan of the S 2p electrons in Figure 3b, deconvolution yielded two pairs of peaks for sulfur in C−S bonds (162.2 and 162.7 eV) and S−S bonds (163.2 and 164.3 eV),[39] which is consistent with those observed with elemental sulfur (Figure S4). Calculations based on the integrated peak areas showed that 26.8 at. % of the sulfur element was in the form of C−S while 73.2 at. % in S−S, which signifies that 16.9 at. % of the total elemental sulfur was directly bonded to P3BT and the remaining 83.1 at. % was subsequently bonded to the sulfurs to form polysulfides. In addition, deconvolution of the high resolution spectrum of the C 1s electrons also yielded two peaks at 283.5 and 284.2 eV (Figure 3c), which may be assigned to S−C, and C−C/C═C bonds, respectively. This confirmed the successful breakage of the S_8 rings and covalent bonding interactions between S and the polymer matrix.

To determine the sulfur content in radical polymers, TGA measurements were then carried out.[3,41] From Figure 3d, it can be seen that the weight loss of pure sulfur started at 150 °C and ended at ca. 300 °C. The CP(S3BT) sample also showed a weight loss of about 70% at 150−300 °C due to the evaporation of sulfur nanocrystals, with P3BT accounting for the remaining 30%. Because the decomposition temperature of sulfur in CP(S3BT) copolymers is very close to that of pure sulfur,[38] these observations clearly showed that the loading of active sulfur was about 70 wt % in CP(S3BT), except for that within the pentagonal thiophene ring.

The copolymerization of sulfur and 3-butylthiophene via the formation of C−S bonds is further verified by FTIR measurements. As shown in Figure 4a, in comparison to the polymer of 3-butylthiophene (P3BT), CP(S3BT) exhibits a new peak at 1720 cm^{-1} that may be assigned to the stretching vibrations of the C−S bond.[42,43] Therefore, the appearance of

DOI: 10.1021/acs.jpcc.6b09543
J. Phys. Chem. C 2017, 121, 2495−2503

this new peak signifies that sulfur has been covalently bonded to 3-butylthiophene. In Figure 4b, nearly identical FTIR spectra can be observed for CP(S3BT) before and after 500 discharge−charge cycles at 1 C. This clearly shows that the C−S bonds between sulfur and 3-butylthiophene were stable even after long-time discharge−charge cycling. This conclusion is further supported by XPS measurement in Figure 4c, where the deconvoluted peaks ascribed to C−S can still be observed after cycling. The formation of these highly stable C−S bonds in CP(S3BT) may help impede the dissolution and diffusion of polysulfides in Li−S battery.

The crystalline structure of CP(S3BT) was then studied by XRD measurements. As depicted in Figure S5, the XRD patterns of the CP(S3BT) composite were almost identical to those of pure sulfur, indicating that sulfur nanocrystals retained their crystal structures after forming covalent bonds with 3-butylthiophene in P3BT. According to the Scherrer's equation, the size of sulfur nanocrystals along the [222] direction is calculated to be about 9.2 nm, which is consistent with the TEM observations in Figure S3. Furthermore, radical copolymer of sulfur and 3-butylthiophene substantially increased the electrical conductivity to 1.5×10^{-7} S cm^{-1} (Table 1), which is even comparable to that of the mixture of S and conductive carbon black (denoted as S/C). In the mixture with conductive carbon black, the electrical conductivity increased by nearly 3 orders of magnitude enhancement from 4.35×10^{-7} to 6.81×10^{-4} S cm^{-1}for CP(S3BT)/C, as compared to S/C. When the CP(S3BT)/C electrode was capped with a thin layer of PEDOT:PSS, the electrical conductivity was further enhanced by a factor of more than 10, which led to increased performance of Li−S battery, as detailed below.[45]

Table 1. Electrical Conductivity (σ) of Different Samples

sample	σ (S cm^{-1})
S[44]	1×10^{-30}
CP(S3BT)	1.50×10^{-7}
S/C	4.35×10^{-7}
CP(S3BT)/C	6.81×10^{-4}
capped CP(S3BT)/C	2.95×10^{-3}

The electrochemical performances of the different electrodes were then evaluated by cyclic voltammetric measurements. As depicted in Figure 5, two pronounced reduction peaks were observed in the negative potential scans for the S/C electrode, where the first peak at ca. + 2.41 V was attributed to the conversion of sulfur to high-order polysulfides (e.g., Li_2S_8 and Li_2S_6) while the second peak at ca. + 1.92 V was due to the further reduction of polysulfides to sulfides (Li_2S).[46] Yet, only one peak at ca. + 2.16 V was observed for the capped CP(S3BT)/C electrode in the negative potential scan, which signified the conversion of sulfur to low-order polysulfides (e.g., Li_2S_2, Li_2S_4, and Li_2S_6) or sulfide (Li_2S) in this electrode during discharging probably due to the formation of cross-linked networks with numerous covalent bonds between sulfur and 3-butylthiophene and the additional confinement of the PEDOT:PSS coating layer. When the electrode potential was swept positively, a peak at ca. + 2.44 V was observed for both samples, which was due to the oxidation of Li_2S to polysulfides (i.e., Li_2S_2, Li_2S_4, Li_2S_6, and Li_2S_8). The position of these three peaks was highly dependent on the potential scan rates. With an increase of the potential scan rates, the two reduction peaks shifted negatively while the oxidation peak positively.

To further understand the electrochemical performance of the cathode materials, EIS study was conducted at the first cycle. As shown in Figure 6, the semicircles observed at high frequencies reflects the electron-transfer resistance (R_{CT}) between the electrode and the electrolyte interfacial layers.[47] It can be seen that the CP(S3BT)/C electrode showed a remarkably reduced R_{CT} of only 111 Ω, as compared to 203 Ω of the S/C electrode. When the CP(S3BT)/C electrode was capped with a thin layer of PEDOT:PSS (i.e., capped CP(S3BT)/C), R_{CT} was further reduced to 100 Ω. The linear segment in the low-frequency region was attributed to the resistance derived from ion diffusion within the electrodes.

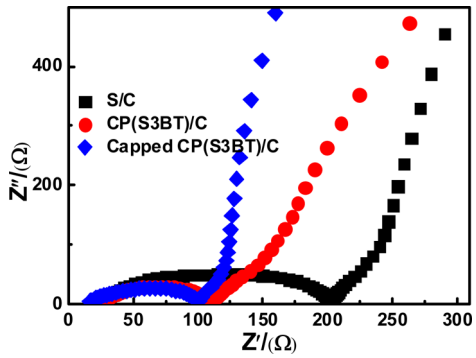

Figure 6. EIS spectra of capped CP(S3BT)/C, CP(S3BT)/C, and S/C electrodes.

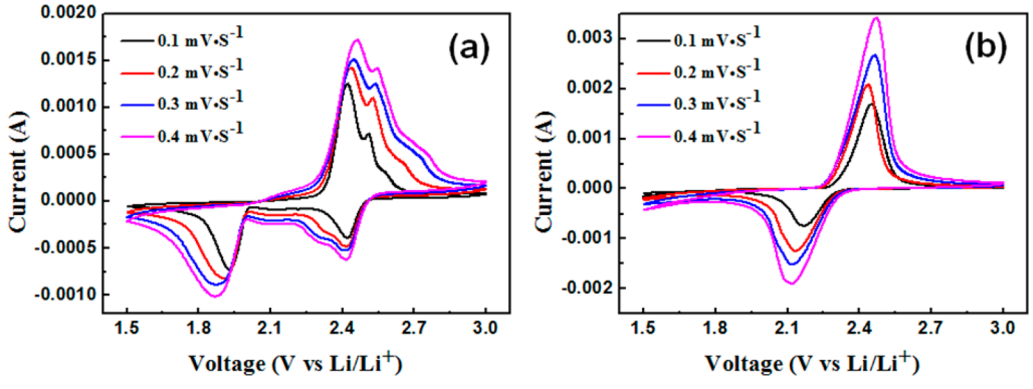

Figure 5. Cyclic voltammograms (CV) of (a) S/C and (b) capped CP(S3BT)/C electrodes in Li−S battery at varied scan rates.

DOI: 10.1021/acs.jpcc.6b09543
J. Phys. Chem. C 2017, 121, 2495−2503

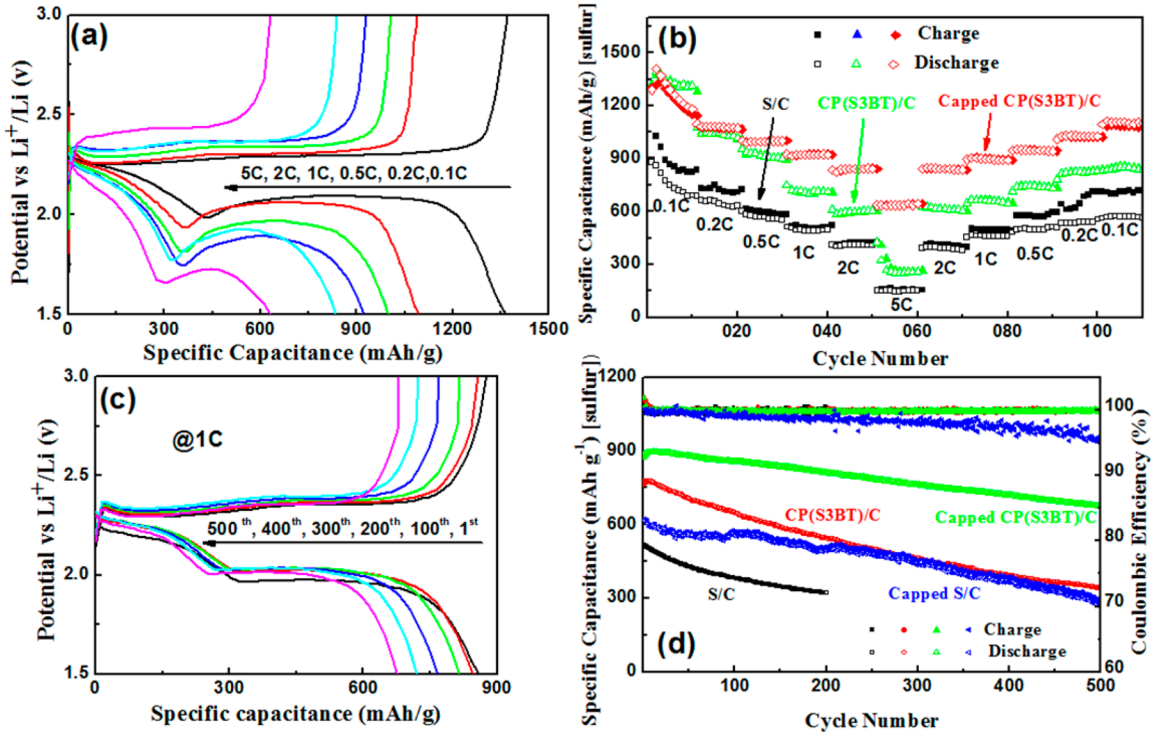

Figure 7. (a) Discharge−charge profiles of capped CP(S3BT)/C cathodes at varied C-rates ranging from 0.1 C to 5 C. (b) Specific capacitance of S/C, CP(S3BT)/C, and capped CP(S3BT)/C cathodes after various numbers of cycles. (c) Discharge−charge profiles of the capped CP(S3BT)/C cathode after various numbers of cycles at 1 C. (d) Cycling performance and Coulombic efficiency of S/C, capped S/C, CP(S3BT)/C and capped CP(S3BT)/C cathodes at 1 C.

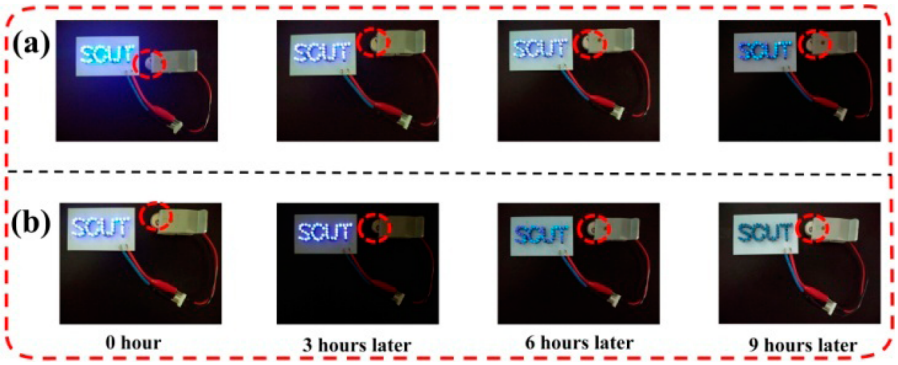

Figure 8. Photographs showing a LED lit by Li−S batteries with different cathode materials: (a) capped CP(S3BT)/C and (b) S/C.

Again a much lower resistance was observed in capped CP(S3BT)/C than those of CP(S3BT)/C and S/C.

To study the electrode stability, the capped CP(S3BT)/C electrode was subjected to cycling tests at various C-rates (Figure 7a,b). The discharge−charge profiles in Figure 7a showed a large discharge capacity in the first cycle, confirming the high conductivity of the capped CP(S3BT)/C electrode. The discharge specific capacities were 1362, 1092, 999, 924, and 835 mA h g^{-1} at 0.1, 0.2, 0.5, 1, and 2 C, respectively. At a much higher C-rate of 5 C, the capped CP(S3BT)/C electrode still showed a specific capacity of 631 mA h g^{-1}. These values were much higher than those observed with the S/C and CP(S3BT)/C cathodes at the same C-rates (Figure S6). Yet, the specific capacity of the capped CP(S3BT)/C electrode was almost completely recovered to the initial value at various C-rates (Figure 7b), indicative of its high reversibility and outstanding rate performance. Figure 7c showed the long-term cycling performance of the above cathodes at 1 C. One can see that although the specific capacity gradually reduced at increasing cycling numbers, the discharging voltages remained almost invariant. In addition, the capped CP(S3BT)/C electrode showed a capacity of 682 mA h g^{-1} even after 500 charge−discharge cycles, while the CP(S3BT) electrode displayed a much lower specific capacity of only 342 mA h g^{-1} and the S/C electrode degraded to 321 mA h g^{-1} after only 200 cycles (Figure 7d). Furthermore, one can see that capping the S/C electrode with a thin layer of PEDOT:PSS polymers increased the capacity to 267 mA h g^{-1} after 500 charge−discharge cycles, which clearly showed the positive effects of copolymerization of sulfur and 3-butylthiophene on the cycling stability of sulfur cathode in Li−S batteries. Remarkably, 99.947% of the capacity of the capped CP(S3BT) electrode was retained in each cycle. Note that increasing the sulfur content in the starting materials to 80 wt % during synthesis led to a

DOI: 10.1021/acs.jpcc.6b09543
J. Phys. Chem. C 2017, 121, 2495−2503

capacitive retention of only 400 mA h g^{-1} after 500 discharge−charge cycles at 1 C (Figure S7), which may be accounted for by increasing phase separation that led to reduced electric conductivity of the cathode and reduced confinement of sulfur by the P3BT blocks.

Note that at the same loading of active sulfur the capped CP(S3BT) electrode showed a much higher capacity and a longer lifespan than the S/C and capped S/C electrodes, signifying that the formation of chemical bonds between sulfur and 3-butylthiophene and the interpenetrating networks of CP(S3BT) effectively impeded the dissolution and diffusion of polysulfides, resulting in remarkable improvement of the cycle performance of Li−S battery. Certainly, for practical applications, the loading of active sulfur needs to be further increased. This will be pursued in future work.

The disparity of the capactive performance was further highlighted with a LED which was powered by Li−S batteries with different cathode materials, as depicted in Figure 8. One can see that the battery with a capped CP(S3BT)/C cathode was able to power the LED even after continuous operation for 9 h while the battery with a S/C cathode ran out of power after only 3 h. This signifies the remarkable enhancement of energy storage of the capped CP(S3BT)/C elecrodeas compared to S/C.

From the above results, one can see that bulk copolymerization of sulfur and 3-butylthiophene substantially enhanced the electrochemical performance of Li−S battery by effectively constraining sulfur during cycling, as compared to pure sulfur cathode. The coating of the bulk copolymer with a thin layer of highly conductive PEDOT:PSS further improved the device performance by additional confinement for polysulfides, leading to excellent cycling stability. Note that the overall performance of the capped CP(S3BT)/C cathode in the present work was better than leading results of polymer or polymer composite cathodes reported recently in the literature (Table S1).[38,48,49] In fact, the method presented herein was proven to be as effective as that reported in recent studies where confinement of sulfur was resorted mostly to carbon-based materials such as porous carbon,[22,50] graphene,[26,51] and carbon fiber.[21,52]

4. CONCLUSION

In summary, bulk copolymers of sulfur and 3-butylthiophene were prepared through radical polymerization by simply heating up the mixture of the two components. Using the thus-prepared copolymer CP(S3BT) as the cathode in Li−S battery, the cycling capacity was substantially enhanced, as compared to S only electrode, which was attributed to (i) physical confinement of sulfur by the P3BT segments in CP(S3BT); and (ii) chemical confinement resulting from covalent bonds between sulfur and 3-butylthiophene in CP(S3BT). Capping the CP(S3BT) with a thin layer of highly conductive PEDOT:PSS remarkably enhanced the conductivity of CP(S3BT), which also helped dramatically increase the C-rate capacity of Li−S battery and retain high cycling stability, with an initial discharge capacity of 1362 mA h g^{-1} at 0.1 C and a retention of 99.947% per cycle in 500 deep charge−discharge cycles. The facile method described herein may offer a new paradigm in the development of cathode electrode materials for efficient and stable Li−S batteries.

■ ASSOCIATED CONTENT

Supporting Information

The Supporting Information is available free of charge on the ACS Publications website at DOI: 10.1021/acs.jpcc.6b09543.

Additional experimental data (PDF)

■ AUTHOR INFORMATION

Corresponding Authors

*(L.L.) E-mail: esguili@scut.edu.cn.

*(S.C.) E-mail: shaowei@ucsc.edu.

ORCID

Ligui Li: 0000-0002-1636-9342

Shaowei Chen: 0000-0002-3668-8551

Notes

The authors declare no competing financial interest.

■ ACKNOWLEDGMENTS

This work was supported by the National Natural Science Foundation of China (NSFC 51402111) and the Fundamental Research Funds for the Central Universities (SCUT Grant No. 2153860). S.C. thanks the National Natural Science Foundation of China (NSFC 21528301) for partial support of the work.

■ REFERENCES

(1) Song, J.; Gordin, M. L.; Xu, T.; Chen, S.; Yu, Z.; Sohn, H.; Lu, J.; Ren, Y.; Duan, Y.; Wang, D. Strong Lithium Polysulfide Chemisorption on Electroactive Sites of Nitrogen-Doped Carbon Composites for High-Performance Lithium-Sulfur Battery Cathodes. *Angew. Chem., Int. Ed.* **2015**, *54*, 4325−4329.

(2) Pope, M. A.; Aksay, I. A. Structural Design of Cathodes for Li-S Batteries. *Adv. Energy Mater.* **2015**, *5*, 1500124.

(3) Chung, W. J.; Griebel, J. J.; Kim, E. T.; Yoon, H.; Simmonds, A. G.; Ji, H. J.; Dirlam, P. T.; Glass, R. S.; Wie, J. J.; Nguyen, N. A.; et al. The Use of Elemental Sulfur as an Alternative Feedstock for Polymeric Materials. *Nat. Chem.* **2013**, *5*, 518−524.

(4) Wang, J.; He, Y. S.; Yang, J. Sulfur-Based Composite Cathode Materials for High-Energy Rechargeable Lithium Batteries. *Adv. Mater.* **2015**, *27*, 569−575.

(5) Larcher, D.; Tarascon, J. Towards Greener and More Sustainable Batteries for Electrical Energy Storage. *Nat. Chem.* **2015**, *7*, 19−29.

(6) Liang, X.; Hart, C.; Pang, Q.; Garsuch, A.; Weiss, T.; Nazar, L. F. A Highly Efficient Polysulfide Mediator for Lithium-Sulfur Batteries. *Nat. Commun.* **2015**, *6*, 5682.

(7) Li, G. C.; Li, G. R.; Ye, S. H.; Gao, X. P. A Polyaniline-Coated Sulfur/Carbon Composite with an Enhanced High-Rate Capability as a Cathode Material for Lithium/Sulfur Batteries. *Adv. Energy Mater.* **2012**, *2*, 1238−1245.

(8) Ji, X.; Nazar, L. F. Advances in Li-S Batteries. *J. Mater. Chem.* **2010**, *20*, 9821−9826.

(9) Wang, H.; Yang, Y.; Liang, Y.; Robinson, J. T.; Li, Y.; Jackson, A.; Cui, Y.; Dai, H. Graphene-Wrapped Sulfur Particles as a Rechargeable Lithium-Sulfur Battery Cathode Material with High Capacity and Cycling Stability. *Nano Lett.* **2011**, *11*, 2644−2647.

(10) Wei Seh, Z.; Li, W.; Cha, J. J.; Zheng, G.; Yang, Y.; McDowell, M. T.; Hsu, P.-C.; Cui, Y. Sulphur-TiO_2 Yolk-Shell Nanoarchitecture with Internal Void Space for Long-Cycle Lithium-Sulphur Batteries. *Nat. Commun.* **2013**, *4*, 1331−1336.

(11) Liu, N.; Lu, Z.; Zhao, J.; McDowell, M. T.; Lee, H.-W.; Zhao, W.; Cui, Y. A Pomegranate-Inspired Nanoscale Design for Large-Volume-Change Lithium Battery Anodes. *Nat. Nanotechnol.* **2014**, *9*, 187−192.

(12) Su, Y.-S.; Fu, Y.; Cochell, T.; Manthiram, A. A Strategic Approach to Recharging Lithium-Sulphur Batteries for Long Cycle Life. *Nat. Commun.* **2013**, *4*, 2985 DOI: 10.1038/ncomms3985.

(13) Borchardt, L.; Oschatz, M.; Kaskel, S. Carbon Materials for Lithium Sulfur Batteries-Ten Critical Questions. *Chem. - Eur. J.* **2016**, *22*, 7324.
(14) Elazari, R.; Salitra, G.; Garsuch, A.; Panchenko, A.; Aurbach, D. Sulfur-Impregnated Activated Carbon Fiber Cloth as a Binder-Free Cathode for Rechargeable Li-S Batteries. *Adv. Mater.* **2011**, *23*, 5641−5644.
(15) Zhou, G.; Wang, D.-W.; Li, F.; Hou, P.-X.; Yin, L.; Liu, C.; Lu, G. Q. M.; Gentle, I. R.; Cheng, H.-M. A Flexible Nanostructured Sulphur-Carbon Nanotube Cathode with High Rate Performance for Li-S Batteries. *Energy Environ. Sci.* **2012**, *5*, 8901−8906.
(16) Yang, X.; Yu, Y.; Yan, N.; Zhang, H.; Li, X.; Zhang, H. 1-D Oriented Cross-Linking Hierarchical Porous Carbon Fibers as a Sulfur Immobilizer for High Performance Lithium-Sulfur Batteries. *J. Mater. Chem. A* **2016**, *4*, 5965−5972.
(17) Singhal, R.; Chung, S.-H.; Manthiram, A.; Kalra, V. A Free-Standing Carbon Nanofiber Interlayer for High-Performance Lithium-Sulfur Batteries. *J. Mater. Chem. A* **2015**, *3*, 4530−4538.
(18) Chung, S. H.; Han, P.; Singhal, R.; Kalra, V.; Manthiram, A. Electrochemically Stable Rechargeable Lithium-Sulfur Batteries with a Microporous Carbon Nanofiber Filter for Polysulfide. *Adv. Energy Mater.* **2015**, *5*, 1500738.
(19) Qie, L.; Chen, W.; Xu, H.; Xiong, X.; Jiang, Y.; Zou, F.; Hu, X.; Xin, Y.; Zhang, Z.; Huang, Y. Synthesis of Functionalized 3d Hierarchical Porous Carbon for High-Performance Supercapacitors. *Energy Environ. Sci.* **2013**, *6*, 2497−2504.
(20) Chen, R.; Zhao, T.; Lu, J.; Wu, F.; Li, L.; Chen, J.; Tan, G.; Ye, Y.; Amine, K. Graphene-Based Three-Dimensional Hierarchical Sandwich-Type Architecture for High-Performance Li/S Batteries. *Nano Lett.* **2013**, *13*, 4642−4649.
(21) Wang, H.; Zhang, W.; Liu, H.; Guo, Z. A Strategy for Configuration of an IntegratedFlexible Sulfur Cathode for High-Performance Lithium-Sulfur Batteries. *Angew. Chem., Int. Ed.* **2016**, *55*, 3992−3996.
(22) Qie, L.; Manthiram, A. A Facile Layer-by-Layer Approach for High-Areal-CapacitySulfur Cathodes. *Adv. Mater.* **2015**, *27*, 1694−1700.
(23) Song, J.; Xu, T.; Gordin, M. L.; Zhu, P.; Lv, D.; Jiang, Y. B.; Chen, Y.; Duan, Y.; Wang, D. Nitrogen-Doped Mesoporous Carbon Promoted Chemical Adsorption of Sulfur and Fabrication of High-Areal-Capacity Sulfur Cathode with Exceptional Cycling Stability for Lithium-Sulfur Batteries. *Adv. Funct. Mater.* **2014**, *24*, 1243−1250.
(24) Chang, C. H.; Chung, S. H.; Manthiram, A. Effective Stabilization of a High-Loading Sulfur Cathode and a Lithium-Metal Anode in Li-S Batteries Utilizing Swcnt-Modulated Separators. *Small* **2016**, *12*, 174−179.
(25) Su, Y.-S.; Manthiram, A. A New Approach to Improve Cycle Performance of Rechargeable Lithium-Sulfur Batteries by Inserting a Free-Standing Mwcnt Interlayer. *Chem. Commun.* **2012**, *48*, 8817−8819.
(26) Huang, J.-Q.; Zhuang, T.-Z.; Zhang, Q.; Peng, H.-J.; Chen, C.-M.; Wei, F. PermselectiveGraphene Oxide Membrane for Highly Stable and Anti-Self-Discharge Lithium-Sulfur Batteries. *ACS Nano* **2015**, *9*, 3002−3011.
(27) Xu, C.; Wu, Y.; Zhao, X.; Wang, X.; Du, G.; Zhang, J.; Tu, J. Sulfur/Three-Dimensional Graphene Composite for High Performance Lithium-Sulfur Batteries. *J. Power Sources* **2015**, *275*, 22−25.
(28) He, J.; Chen, Y.; Li, P.; Fu, F.; Wang, Z.; Zhang, W. Three-Dimensional Cnt/Graphene-Sulfur Hybrid Sponges with High Sulfur Loading as Superior-Capacity Cathodes for Lithium-Sulfur Batteries. *J. Mater. Chem. A* **2015**, *3*, 18605−18610.
(29) Zhou, G.; Zhao, Y.; Manthiram, A. Dual-Confined Flexible Sulfur Cathodes Encapsulated in Nitrogen-Doped Double-Shelled Hollow Carbon Spheres and Wrapped with Graphene for Li-S Batteries. *Adv. Energy Mater.* **2015**, *5*, 1402263.
(30) Xiao, L.; Cao, Y.; Xiao, J.; Schwenzer, B.; Engelhard, M. H.; Saraf, L. V.; Nie, Z.; Exarhos, G. J.; Liu, J. A Soft Approach to Encapsulate Sulfur: Polyaniline Nanotubes for Lithium-Sulfur Batteries with Long Cycle Life. *Adv. Mater.* **2012**, *24*, 1176−1181.
(31) Zeng, F.; Wang, W.; Wang, A.; Yuan, K.; Jin, Z.; Yang, Y.-s. Multidimensional Polycation B-Cyclodextrin Polymer as an Effective Aqueous Binder for High Sulfur Loading Cathode in Lithium-Sulfur Batteries. *ACS Appl. Mater. Interfaces* **2015**, *7*, 26257−26265.
(32) Fu, Y.; Manthiram, A. Enhanced Cyclability of Lithium-Sulfur Batteries by a Polymer Acid-Doped Polypyrrole Mixed Ionic-Electronic Conductor. *Chem. Mater.* **2012**, *24*, 3081−3087.
(33) Bhattacharya, P.; Nandasiri, M. I.; Lv, D.; Schwarz, A. M.; Darsell, J. T.; Henderson, W. A.; Tomalia, D. A.; Liu, J.; Zhang, J.-G.; Xiao, J. Polyamidoamine Dendrimer-Based Binders for High-Loading Lithium-Sulfur Battery Cathodes. *Nano Energy* **2016**, *19*, 176−186.
(34) Liang, X.; Liu, Y.; Wen, Z.; Huang, L.; Wang, X.; Zhang, H. A Nano-Structured and Highly Ordered Polypyrrole-Sulfur Cathode for Lithium-Sulfur Batteries. *J. Power Sources* **2011**, *196*, 6951−6955.
(35) Zheng, J.; Tian, J.; Wu, D.; Gu, M.; Xu, W.; Wang, C.; Gao, F.; Engelhard, M. H.; Zhang, J.-G.; Liu, J.; et al. Lewis Acid-Base Interactions between Polysulfides and Metal Organic Framework in Lithium Sulfur Batteries. *Nano Lett.* **2014**, *14*, 2345−2352.
(36) Liang, X.; Garsuch, A.; Nazar, L. F. Sulfur Cathodes Based on Conductive Mxene Nanosheets for High-Performance Lithium-Sulfur Batteries. *Angew. Chem., Int. Ed.* **2015**, *54*, 3907−3911.
(37) Maldonado-Hodar, F.; Moreno-Castilla, C.; Rivera-Utrilla, J.; Hanzawa, Y.; Yamada, Y. Catalytic Graphitization of Carbon Aerogels by Transition Metals. *Langmuir* **2000**, *16*, 4367−4373.
(38) Oschmann, B.; Park, J.; Kim, C.; Char, K.; Sung, Y.-E.; Zentel, R. Copolymerization of Polythiophene and Sulfur to Improve the Electrochemical Performance in Lithium-Sulfur Batteries. *Chem. Mater.* **2015**, *27*, 7011−7017.
(39) Kim, H.; Lee, J.; Ahn, H.; Kim, O.; Park, M. J. Synthesis of Three-Dimensionally Interconnected Sulfur-Rich Polymers for Cathode Materials of High-Rate Lithium-Sulfur Batteries. *Nat. Commun.* **2015**, *6*, 7278.
(40) Zhang, Z.; Jing, H.-K.; Liu, S.; Li, G.-R.; Gao, X.-P. Encapsulating Sulfur into a Hybrid Porous Carbon/Cnt Substrate as a Cathode for Lithium-Sulfur Batteries. *J. Mater. Chem. A* **2015**, *3*, 6827−6834.
(41) Li, B.; Li, S.; Xu, J.; Yang, S. A New Configured Lithiated Silicon-Sulfur Battery Built on 3d Graphene with Superior Electrochemical Performances. *Energy Environ. Sci.* **2016**, *9*, 2025−2030.
(42) Li, W.; Zhou, M.; Li, H.; Wang, K.; Cheng, S.; Jiang, K. A High Performance Sulfur-Doped Disordered Carbon Anode for Sodium Ion Batteries. *Energy Environ. Sci.* **2015**, *8*, 2916−2921.
(43) Talapaneni, S. N.; Hwang, T. H.; Je, S. H.; Buyukcakir, O.; Choi, J. W.; Coskun, A. Elemental-Sulfur Mediated Facile Synthesis of a Covalent TriazineFramework for High-Performance Lithium-Sulfur Batteries. *Angew. Chem.* **2016**, *128*, 3158−3163.
(44) Li, G. C.; Li, G. R.; Ye, S. H.; Gao, X. P. A Polyaniline-Coated Sulfur/Carbon Composite with an Enhanced High-Rate Capability as a Cathode Material for Lithium/Sulfur Batteries. *Adv. Energy Mater.* **2012**, *2*, 1238−1245.
(45) Abbas, S. A.; Ibrahem, M. A.; Hu, L.-H.; Lin, C.-N.; Fang, J.; Boopathi, K. M.; Wang, P.-C.; Li, L.-J.; Chu, C.-W. Bifunctional Separator as a Polysulfide Mediator for Highly Stable Li-S Batteries. *J. Mater. Chem. A* **2016**, *4*, 9661−9669.
(46) Ji, X.; Lee, K. T.; Nazar, L. F. A Highly Ordered Nanostructured Carbon-Sulphur Cathode for Lithium-Sulphur Batteries. *Nat. Mater.* **2009**, *8*, 500−506.
(47) Cao, R.; Chen, J.; Han, K. S.; Xu, W.; Mei, D.; Bhattacharya, P.; Engelhard, M. H.; Mueller, K. T.; Liu, J.; Zhang, J. G. Effect of the Anion Activity on the Stability of Li Metal Anodes in Lithium-Sulfur Batteries. *Adv. Funct. Mater.* **2016**, *26*, 3059−3066.
(48) Yan, M.; Zhang, Y.; Li, Y.; Huo, Y.; Yu, Y.; Wang, C.; Jin, J.; Chen, L.; Hasan, T.; Wang, B.; Su, B.-L. Manganese dioxide nanosheet functionalized sulfur@PEDOT core-shell nanospheres for advanced lithium-sulfur batteries. *J. Mater. Chem. A* **2016**, *4*, 9403−9412.
(49) Chang, A.; Wu, Q.; Du, X.; Chen, S.; Shen, J.; Song, Q.; Xie, J.; Wu, W. Immobilization of Sulfur in Microgels for Lithium-Sulfur Battery. *Chem. Commun.* **2016**, *52*, 4525−4528.

DOI: 10.1021/acs.jpcc.6b09543
J. Phys. Chem. C 2017, 121, 2495−2503

(50) Jia, X.; Zhang, C.; Liu, J.; Lv, W.; Wang, D. W.; Tao, Y.; Li, Z.; Zheng, X.; Yu, J. S.; Yang, Q. H. Evolution of the Effect of Sulfur Confinement in Graphene-Based Porous Carbons for Use in Li-S Batteries. *Nanoscale* **2016**, *8*, 4447−4451.
(51) Gu, X.; Tong, C.-j.; Lai, C.; Qiu, J.; Huang, X.; Yang, W.; Wen, B.; Liu, L.-m.; Hou, Y.; Zhang, S. A Porous Nitrogen and Phosphorous Dual Doped Graphene Blocking Layer for High Performance Li-S Batteries. *J. Mater. Chem. A* **2015**, *3*, 16670−16678.
(52) Chung, S.-H.; Han, P.; Singhal, R.; Kalra, V.; Manthiram, A. Electrochemically Stable Rechargeable Lithium-Sulfur Batteries with a Microporous Carbon Nanofiber Filter for Polysulfide. *Adv. Energy Mater.* **2015**, *5*, 1500738.

DOI: 10.1021/acs.jpcc.6b09543
J. Phys. Chem. C 2017, 121, 2495−2503